Sulfur-33 NMR at Natural Abundance in Solids

Hellmut Eckert and James P. Yesinowski*

Contribution Number 7311, Southern California Regional NMR Facility, Division of Chemistry and Chemical Engineering, California Institute of Technology, Pasadena, California 91125.
Received September 24, 1985

Abstract: The first detailed study of ^{33}S NMR in the solid state has been carried out for a variety of metal sulfides and sulfates, including naturally occurring minerals. The difficulties inherent with ^{33}S NMR at natural isotopic abundance can be overcome by using a very high magnetic field strength (11.74 T) in order to minimize second-order nuclear quadrupole coupling effects and by employing a RIDE (RIngDown Elimination) pulse sequence to eliminate the severe problem of acoustic ringing. Modification of this sequence by introducing composite pulses enables observation of a significantly larger chemical shift range. Metal sulfates, including the alums, show evidence of second-order quadrupolar broadening effects, from which nuclear electric quadrupolar coupling constants ranging from 0.5 to 2.2 MHz are calculated. The sulfate chemical shifts (330 ppm downfield from CS_2) are nearly identical and are close to the value measured in solution. In contrast, a large chemical shift range (ca. 600 ppm) is observed for the metal sulfides. For ZnS and CdS, both of which occur in the wurtzite structure, $\Delta\sigma$ values of 23 and 28 ppm, respectively, are determined. The explanation of the chemical shift trends in the metal sulfides involves more than simple electronegativity arguments. It is necessary to consider both crystalline ionicities, as measured from dielectric constants, and the effects of orbital overlap. The more covalently bonded post-transition-metal sulfides (ZnS, CdS, and PbS) are appropriately described in terms of the bond orbital model formulated by Harrison. The order of the chemical shifts found for these compounds agrees with that predicted from crystalline ionicities and bond polarity parameters, with the calculated values of the average excitation energy being in a reasonable range. For the alkali and alkaline earth sulfides an extended Kondo-Yamashita approach provides the appropriate description; as observed previously for the alkali halides the shift trends can be rationalized in terms of changes in the anion-cation and anion-anion overlap integrals. The temperature dependence of the chemical shift has been measured for a number of compounds and supports the above conclusions.

Sulfur compounds present a multitude of intriguing problems in different areas of solid-state chemistry. Sulfides and sulfates of virtually every metallic element form naturally occurring minerals, and much geochemical research interest has been devoted to understanding the composition of hydrothermal solutions, the precipitation of minerals, and the sulfide/sulfate equilibria involved prior to or during the formation of minerals.[1] The sulfides are also of interest from the point of view of structural chemistry, since they form a large variety of lattice types, ranging from simple cubic densely packed structures to highly covalent and anisotropic arrangements. In addition, sulfides are important in materials science, the interest focusing on (1) the semiconductor characteristics, (2) the infrared transparency, and (3) the electroluminescent and photoluminescent properties. Large deviations from stoichiometric compositions and an inherent tendency to form solid solutions, both of which are associated with substantial changes in the electronic properties, offer the opportunity to adapt the physicochemical characteristics of a given material to the demands of technological applications.

In view of the rapid development of solid-state NMR methods as a powerful tool in solid-state chemistry and geochemistry as well as in materials science,[2-4] it might seem surprising that the magnetic moment of the ^{33}S isotope ($I = {}^3/_2$) has rarely been utilized. Indeed, the only literature data are repeated measurements of the chemical shift and line width of sphalerite, ZnS.[5-8] In addition, ^{33}S resonances in paramagnetic α-MnS[9] and ferromagnetic EuS[10] have been reported. This paucity of experimental data is due to the unfavorable NMR characteristics of this nuclide, as reflected by a small magnetogyric ratio ($\gamma = 2.055 \times 10^7$ rad T^{-1} s^{-1}), a low natural abundance (0.76%) and a moderate quadrupole moment. Since the NMR signals may be broadened beyond detectability by the presence of even minor field gradients at the sulfur nucleus, only sulfur atoms which are localized in sites of particularly high symmetry can be studied. Even in these cases, only the central ${}^1/_2 \rightarrow {}^{-1}/_2$ transition may be observable in a polycrystalline sample. The line width arising from the broadening effect of the second-order quadrupolar interaction upon this transition decreases proportional to the increase in Larmor frequency.[11] Thus, it is advantageous to operate at the highest possible field strengths, quite apart from any sensitivity considerations.

We report here the results of the first systematic study of ^{33}S NMR in selected solids, carried out at a field of 11.74 T for a variety of polycrystalline sulfides and sulfates, including natural minerals.[12] A detailed discussion of the pulse sequence crucial for obtaining the solid-state ^{33}S NMR spectra will be given. Many of the metal sulfides investigated here belong to the group of binary average valence IV compounds with simple crystal structures for which detailed unified bonding concepts have been developed.[13-20] In the past a number of chemical shift data for such binary compounds have been obtained and interpreted in terms of their bonding properties.[21-35] While the results of these studies provide

(1) Janecki, D. R.; Seyfried, W. E., Jr. *Geochim. Cosmochim. Acta* **1984**, *48*, 2723.
(2) For a review, see: Fyfe, C. A. "Solid State NMR for Chemists"; C.F.C. Press: Guelph, Ontario, Canada.
(3) Oldfield, E.; Kirkpatrick, R. J. *Science* **1985**, *227*, 1537.
(4) Mehring, M. In "NMR-Basic Principles and Progress"; Diehl, P., Fluck, E., Kosfeld, R., Eds.; Springer-Verlag: Berlin, Heidelberg, New York, 1976.
(5) Haller, M.; Hertler, W. E.; Lutz, O.; Nolle, A. *Solid State Commun.* **1980**, *33*, 1051.
(6) Retcofsky, H. L.; Friedel, R. A. *J. Am. Chem. Soc.* **1972**, *94*, 6579.
(7) Karr, C., Jr.; Schultz, H. D. *Spectrosc. Lett.* **1968**, *1*, 205.
(8) Lutz, O. *NATO ASI Ser., Ser. C* **1983**, *103*, 389.
(9) Lee, K. *Phys. Rev.* **1968**, 172, 284.
(10) Suzuki, H.; Komaru, T.; Hihara, T.; Koi, Y. *J. Phys. Soc. Jpn.* **1971**, *30*, 288.
(11) Casabella, P. A. *J. Chem. Phys.* **1964**, *40*, 149.
(12) Eckert, H.; Yesinowski, J. P., Poster presented at the 25th Experimental NMR Conference, Asilomar, CA, April 1985.
(13) Pauling, L. *J. Am. Chem. Soc.* **1932**, *54*, 3570.
(14) Mulliken, R. S. *J. Chem. Phys.* **1934**, *2*, 782.
(15) Gordy, W. *Phys. Rev.* **1946**, *69*, 604.
(16) Phillips, J. C. *Rev. Mod. Phys.* **1970**, *42*, 317.
(17) Van Vechten, J. A. *Phys. Rev.* **1969**, *182*, 891.
(18) Stiles, P. J. *Solid State Commun.* **1972**, *11*, 1063.
(19) Harrison, W. A. *Phys. Rev. B* **1973**, *8*, 4487.
(20) Harrison, W. A.; Ciraci, S. *Phys. Rev. B* **1974**, *10*, 1516.
(21) Koch, W.; Lutz, O.; Nolle, A. *Z. Phys. A* **1978**, *289*, 17.
(22) Turner, G. L.; Chung, S. E.; Oldfield, E. *J. Magn. Reson.* **1985**, *64*, 316.
(23) Sears, R. E. J. *J. Chem. Phys.* **1974**, *61*, 4368.
(24) Kondo, J.; Yamashita, J. *J. Phys. Chem. Solids* **1959**, *10*, 245.
(25) Yosida, K.; Moriya, T. *J. Phys. Soc. Jpn.* **1956**, *11*, 33.
(26) Vaughan, R. W.; Elleman, D. D.; Rhim, W. K.; Stacey, L. M. *J. Chem. Phys.* **1972**, *57*, 5383.

0002-7863/86/1508-2140$01.50/0

Table I. Origin and NMR Parameters of the Compounds Studied

compound[a] (structure)	origin	δ_{iso},[b] ppm	$d\delta_{iso}/dT$, ppm/K	$\Delta\nu_{1/2}$,[c] Hz	e^2qQ/h,[d] MHz
Li_2S } (fluorite)	ALFA, 99.9%	−347		1380	
Na_2S } (fluorite)	ALFA, 99%	−338		500	
MgS	ALFA, technical grade	−174	0.022 ± 0.005	300	
CaS	ALFA, 98%	−28.5	0.011 ± 0.002	100	
SrS	ALFA, 98%	+42.8		100	
BaS (rock salt)	ALFA, 98%	+291	0.007 ± 0.009	250	
PbS*	galena, Picher, Oklahoma	−297	0.116 ± 0.003	580	
PbS*	galena, Kansas	−293		300	
ZnS* (zinc blende)	sphalerite, 1% Fe, Picher, Oklahoma	−228	0.047 ± 0.005	800	
ZnS } (wurtzite)	MCB	−231[e]			
CdS } (wurtzite)	Aldrich, Gold Label, 99.9%	−284[f]	0.040 ± 0.005		
Na_2SO_4*	thenardite } Soda Lake,	+330 ± 3		2300	0.82
$Na_2Ca(SO_4)_2$*	glauberite } S. Luis Obispo	+338 ± 3		1700	0.71
$Na_2Mg(SO_4)_2{\cdot}4H_2O$*	bloedite } County, CA	+321 ± 20		16000 ± 3000	2.2
$CaSO_4$*	anhydrite, New Brunswick	+326 ± 5		3500	1.0
$CaSO_4{\cdot}2H_2O$*	gypsum	+337 ± 3		2000	0.77
$BaSO_4$*	barite, Bullien Mts.			18000 ± 5000	2.3
K_2SO_4	MALLINCKRODT	+334 ± 3		4300	1.13
Rb_2SO_4	ALFA, 99%	+329 ± 3		3500	1.01
Cs_2SO_4	ALFA, 98%	+335 ± 3		3200	0.97
Tl_2SO_4	ALFA, 99.5%	+320 ± 3		3600	1.03
$(NH_4)_2SO_4$	BAKER, 99.7%	+328 ± 3		1200	0.59
$KAl(SO_4)_2{\cdot}12H_2O$	synthesized	+327 ± 2		2100	0.79
$RbAl(SO_4)_2{\cdot}12H_2O$	synthesized	+334 ± 2		1050	0.56
$CsAl(SO_4)_2{\cdot}12H_2O$	synthesized	+331 ± 2		950	0.53
$NH_4Al(SO_4)_2{\cdot}12H_2O$	synthesized	+333 ± 2		950	0.53
$TlAl(SO_4)_2{\cdot}12H_2O$	synthesized	+332 ± 2		1050	0.56

[a] Mineral samples are designated by an asterisk. [b] ±1 ppm unless specified, referenced to CS_2. [c] ±10% unless specified. [d] Upper limit. [e] $\Delta\sigma$ = +23 ppm. [f] $\Delta\sigma$ = +28 ppm.

useful comparisons with the present study, previous discussions of the chemical shifts have been somewhat limited by the absence of an absolute chemical shift scale, as well as by a limited range of compound structural types. An absolute shift scale for ^{33}S NMR has recently been established,[36] which enables us to obtain further quantitative information from chemical shifts and their temperature dependencies. In addition, the wide range of structural types we have studied leads us to consider several different approaches for explaining chemical shift trends and results in some clarification of the various factors responsible.

Experimental Section

Table I lists the origin of all the samples investigated in the present study. The mineral samples were kindly provided by Prof. George Rossman, Division of Geological and Planetary Sciences, CIT. Most of the other compounds were obtained commercially, while the alums were synthesized following the general procedure outlined in ref 37. Most NMR spectra were obtained at ambient temperature, while PbS, MgS, CaS, BaS, CdS, and ZnS were studied over the temperature range 300–400 K.

All measurements were carried out on a BRUKER WM-500 low-power high-resolution spectrometer, equipped with a 10 mm broadband low-γ probe, at an operating frequency of 38.372 MHz. Spectra obtained conventionally, using single pulses, were severely impaired by the appearance of a "rolling base line", an artifact arising from acoustic ringing in the probe, pulse breakthrough, and filter response.[38,39] In the past, several acquisition algorithms have been proposed to alleviate this problem.[40-43] Most recently, a highly effective pulse sequence called RIDE

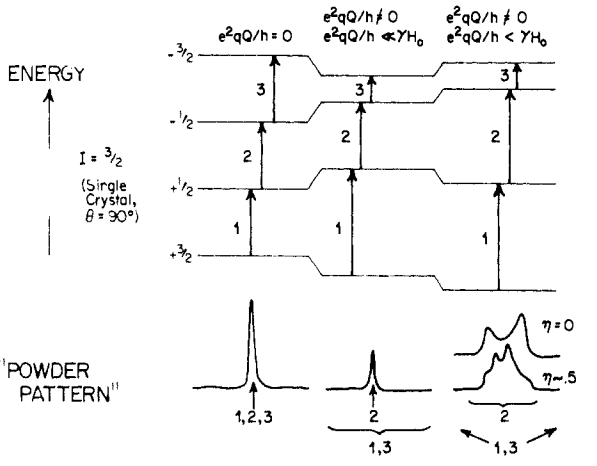

Figure 1. Energy-level diagram and typical NMR line shapes observed in polycrystalline solids arising from quadrupolar perturbations of $I = {}^3/_2$ nuclei.

("RIngDown Elimination") has been introduced which combines phase cycling with inverted signal subtraction.[44,45] The sequence is as follows

$90°_x$--add--$90°_{-x}$--subtract--$180°_x$-- ×

D1--$90°_{-x}$--add--$180°_x$--D1--$90°_x$--subtract

where "add" and "subtract" refer to how the free induction decay acquired is placed into memory.

In the present work resonance offsets were found to degrade severely the performance of the RIDE sequence because of the relatively low pulse power used. Therefore the $180°_x$ pulses were replaced by $90°_x$–$180°_y$–$90°_x$ composite pulses[46,47] in order to achieve a wider range of effective excitation. Since these composite pulses also compensate for radio frequency field inhomogeneities and flip angle missetting, the sensitivity is

(27) Willig, A.; Sapoval, B. *J. Phys. Lett.* **1977**, *38*, L-57.
(28) Willig, A.; Sapoval, B.; Leibler, K.; Verie, C. *J. Phys. C* **1976**, *9*, 1981.
(29) Senturia, S. D.; Smith, A. C.; Hewes, C. R.; Hofmann, J. A.; Sagalyn, P. L. *Phys. Rev. B* **1970**, *1*, 4045.
(30) Guenther, B. D.; Hultsch, R. A. *J. Magn. Reson.* **1969**, *1*, 609.
(31) Mebs, R. W.; Carter, G. C.; Evans, B. J.; Bennett, L. H. *Solid State Commun.* **1972**, *10*, 769.
(32) Sears, R. E. J. *Phys. Rev. B.* **1978**, *18*, 3054.
(33) Sears, R. E. J. *Phys. Rev. B* **1980**, *22*, 1135.
(34) Bogdanov, V. L.; Lemanov, V. V. *Fiz. Tverd. Tela* **1968**, *10*, 286.
(35) Luetgemeier, H. Z. *Naturforsch. A* **1964**, *19*, 1297.
(36) Wasylishen, R. E.; Connor, C.; Friedrich, J. O. *Can. J. Chem. A.* **1984**, *62*, 981.
(37) Haussuehl, S. *Z. Kristallogr.* **1961**, *116*, 371.
(38) Buess, M. L.; Petersen, G. L. *Rev. Sci. Instrum.* **1978**, *49*, 1151.
(39) Fukushima, E.; Roeder, S. B. W. *J. Magn. Reson.* **1979**, *33*, 199.
(40) Hoult, D. J.; Chen, C. N.; Eden, H.; Eden, M. *J. Magn. Reson.* **1983**, *51*, 110.
(41) Canet, D.; Brondeau, J.; Marchal, J. P.; Robin-Lherbier, B. *Org. Magn. Reson.* **1982**, *20*, 51.
(42) Patt, S. L. *J. Magn. Reson.* **1982**, *49*, 161.
(43) Fukushima, E.; Roeder, S. B. W. "Experimental Pulse NMR"; Addison Wesley Pub. Comp. Inc.: Reading, MA, 1981.
(44) Ellis, P. D., Discussion at the NATO Meeting Advanced Study Institute on Multinuclear NMR Spectroscopy, Stirling, August 1981.
(45) Belton, P. S.; Cox, I. J.; Harris, R. K. *J. Chem. Soc., Faraday Trans. 2* **1985**, *81*, 63.
(46) Levitt, M. H.; Freeman, R. *J. Magn. Reson.* **1979**, *33*, 473.
(47) Freeman, R.; Kempsell, S. P.; Levitt, M. H. *J. Magn. Reson.* **1980**, *38*, 453.

improved as well. No attempt was made to use composite 90° pulses or other types of composite 180° pulses since the above sequence worked satisfactorily. The ringdown delay D1 following the composite 180° pulse was optimized by systematic variation; a value of 100 μs was appropriate for most of the compounds studied. Typical acquisition parameters were the following: spectral width 100 kHz, 4K data points, 90° pulse width (for liquid CS_2) 53 μs. A relaxation delay of 20–60 s after each acquisition was used. This last parameter was chosen for various types of samples to roughly optimize the signal/noise ratio. It illustrates the fairly long spin–lattice relaxation times in these solids (the alums and PbS are clearly the best solid-state test samples in this respect, with repetition intervals of a few seconds being possible). All free induction decays were acquired unlocked, in nonspinning samples, processed without left shifting and multiplied by an exponential digital filter function prior to Fourier transformation.

Results and Data Analysis

NMR spectra of ^{33}S in the solid state are expected to be dominated by the static interaction of the nuclear quadrupole moment with electric field gradients arising from noncubic electronic environments. As shown in Figure 1 this removes the energetic equivalence of the three Zeeman transitions observed for an $I = {}^3/_2$ nucleus, leaving the central ${}^1/_2 \rightarrow -{}^1/_2$ transition unaffected, as long as the ratio of the quadrupolar interaction energy to the energy of the Zeeman interaction is smaller than ca. 0.05 ("first-order spectra"). The "satellite" transitions ${}^3/_2 \rightarrow {}^1/_2$ and $-{}^1/_2 \rightarrow -{}^3/_2$ occur over a considerable spectral range in a polycrystalline sample and are frequently not observable. If the energy ratio mentioned above becomes larger than 0.05, the frequency of the central transition becomes noticeably dependent upon the quadrupolar coupling constant. In a polycrystalline sample powder patterns such as shown on the bottom right of Figure 1 result. The exact shape depends on the magnitude of the asymmetry parameter, η. In general, the quadrupolar Hamiltonian parameters, e^2qQ/h and η, can be extracted from these line shapes via computer simulation,[48] while for the special case of $\eta = 0$ the quadrupole coupling constant follows from the frequency separation Γ of singularities (shown in Figure 1) according to the formula[11]

$$\frac{e^2qQ}{h} = \left(\frac{192\nu_0\Gamma}{25}\right)^{1/2} \qquad (1)$$

where ν_0 denotes the Larmor frequency.

Figure 2 shows some representative spectra obtained from the present samples. The results obtained are summarized in Figure 3 and Table I. It has been shown theoretically that the 90° pulse length for the central transition of an $I = {}^3/_2$ nucleus becomes ${}^1/_2$ of the normal value (as measured in a liquid) when the satellite transitions are not excited by the radio frequency pulse.[49] We observe this behavior in all solids studied in the present work, which implies that only the central ${}^1/_2 \rightarrow -{}^1/_2$ transition is being excited. For the cubic sulfides this may be rationalized in terms of lattice defects or motional/vibrational degrees of freedom which produce nonzero field gradients at the sulfur nucleus. The central transitions of wurtzite-type ZnS and CdS (which also crystallizes in the wurtzite structure) resemble the familiar powder patterns arising from an axially symmetric chemical shift tensor, suggesting that at the operating frequency of 38.372 MHz the shift anisotropy dominates over the second-order quadrupole broadening. The chemical shift anisotropy, as extracted from the inflection points of the respective powder patterns, amounts to 23 (±1) and 28 (±1) ppm for ZnS (wurtzite) and CdS, respectively. The stated error limits neglect possible contributions from the second-order quadrupole broadening. This compares to the value of 44 ppm for ^{77}Se in wurtzite-type CdSe, as determined from the powder pattern by Lutz and co-workers.[21]

Table I shows that ^{33}S NMR can distinguish between the two crystallographic forms of ZnS, sphalerite and wurtzite. Also, the

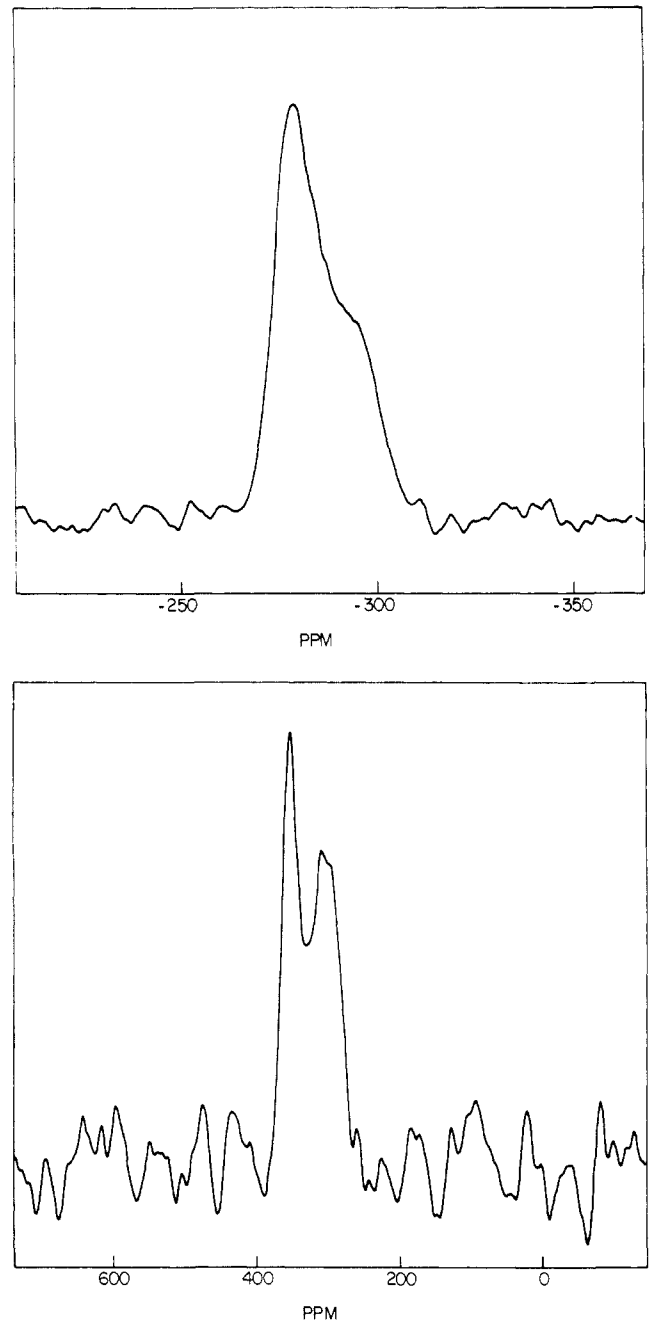

Figure 2. (A, top) Solid-state ^{33}S NMR spectrum of cadmium sulfide, 2080 transients, 20-s pulse repetition interval, 100-Hz line broadening. (B, bottom) Solid-state ^{33}S NMR spectrum of cesium sulfate, 680 transients, 60-s pulse repetition interval, 500-Hz line broadening.

comparison of the data obtained for two mineral samples of PbS (galena) from different origins showed slight differences in line widths and chemical shifts, possibly due to minor differences in composition and/or lattice defects.

In contrast to the sulfides, the spectra of many of the sulfates show clear indications of second-order quadrupolar broadening. In principle the quadrupolar Hamiltonian parameters could be evaluated from these powder patterns; however, for the present compounds, the signal-to-noise ratios obtainable were not large enough to permit an unequivocal determination. Thus, application of eq 1 to the observed singularities will lead to underestimates of the coupling constant when η is nonzero. A better approach, especially in the case of unresolved lines, is to approximate Γ in eq 1 by the full width at half-height of the overall line shape. The estimated quadrupolar coupling constants listed in Table I are thus to be considered crude approximate values, and the presence of additional broadening mechanisms (chemical shift anisotropy, dipolar coupling) would make them overestimates. The e^2qQ/h

(48) Baugher, J. F.; Kriz, M. H.; Taylor, P. C.; Bray, P. J. *J. Magn. Reson.* **1970**, *3*, 415.
(49) Abragam A. "The Principles of Nuclear Magnetism"; Clarendon Press: Oxford, 1967; p 37.

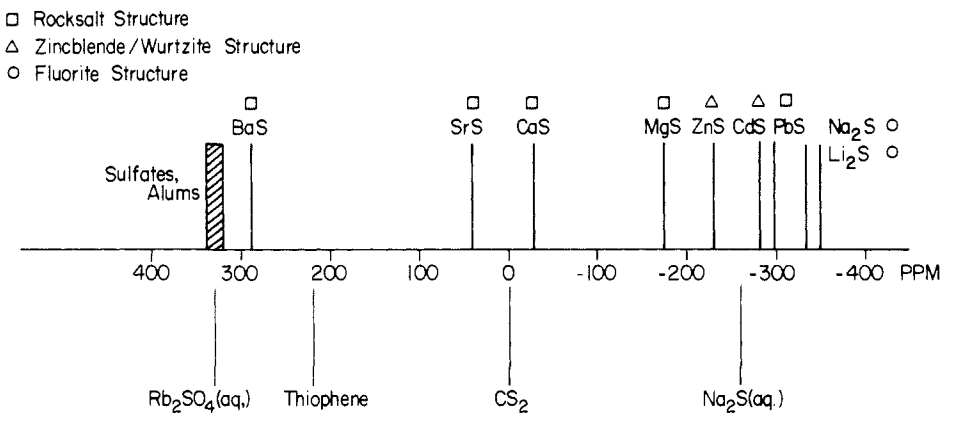

Figure 3. ^{33}S NMR chemical shifts in solids, with some solution-state references for comparison.

values thus calculated were subsequently used to obtain corrected chemical shift data from the measured line positions[11] (see Table I).

Discussion

Chemical Shifts and Nuclear Quadrupolar Coupling Constants in Metal Sulfates. The present study shows that the local symmetry of the sulfur nucleus in sulfates, represented by a more or less ideal tetrahedral oxygen coordination, is high enough to permit a facile detection of the ^{33}S NMR signal in a large variety of unlabeled materials at 11.74 T. As can be seen from Table I the chemical shifts of the sulfates show almost no variations appreciably outside of experimental error, the only noticeable exception being for Tl_2SO_4, which is shifted significantly upfield with respect to its isostructural homologues. In contrast to the similarity of chemical shifts, the quadrupolar coupling constants show large variations which appear to reflect differences in the crystal structures. The heavier Ia sulfates (including thallous sulfate), all of which crystallize in the orthorhombic K_2SO_4 structure,[50] show almost identical second-order quadrupolar powder patterns. With the exception of $(NH_4)_2SO_4$ all of the latter compounds exhibit a uniform quadrupole coupling constant of ca. 1.2 MHz. Similarities also occur within the group of the cubic alums, for which the observation of second-order quadrupole effects can be rationalized in terms of slight displacements of the SO_4 tetrahedra from a cubic environment within the unit cell.[51] While the quadrupole coupling constant of $KAl(SO_4)_2 \cdot 12H_2O$ stands out significantly from the others (for unknown reasons), the subtle structural differences between α- and β-alums[37] are not reflected in the ^{33}S NMR spectra. However, other types of structural and compositional differences change the quadrupole coupling constant markedly, cf. anhydrite ($CaSO_4$) and gypsum ($CaSO_4 \cdot 2H_2O$), or the sodium sulfates thenardite, glauberite, and bloedite. Furthermore, barite ($BaSO_4$) and celestite ($SrSO_4$), in both of which the coordination of the sulfate tetrahedra by the counterion is less well defined,[52] show very broad lines (ca. 15 kHz) which are beyond the limit of uniform radio frequency excitation. No simple correlation exists between the quadrupole coupling constants and the valency of the counterions.

General Chemical Shift Trends among Metal Sulfides. The range of ^{33}S chemical shifts in liquids has been discussed extensively, and an approximate absolute scale has been derived.[36] Li_2S and Na_2S, both of which crystallize in the antifluorite structure, are significantly shifted upfield with respect to an aqueous solution of sodium sulfide[6] and show the largest upfield values ever reported for any sulfur compound, corresponding to respective shielding values of 928 and 919 ppm on the absolute chemical shift scale proposed by Wasylishen and co-workers[36] (on which our reference compound CS_2 resonates 581-ppm upfield). If we estimate the diamagnetic contribution σ_{dia} to the shielding in Li_2S to be that in H_2S, 1066.7 ppm,[53] then we can use the Ramsey formula for chemical shifts[54]

$$\sigma = \sigma_{dia} + \sigma_{para} \quad (2)$$

Table II. Parameters for Absolute Shift Calculations of the Post-Transition-Metal Sulfides

compd	$-\sigma_p$,[a] ppm	α_p	$u^2(1-u^2)$		Δ, eV	
			$S=0$	$S=S_{max}$[b]	$S=0$	$S=S_{max}$[b]
ZnS	258	0.73	0.1168	0.1483	3.4	4.2
CdS	202	0.77	0.1017	0.1304	3.8	4.7
PbS	189	0.79[c]	0.0939	0.1209	3.7	4.7

[a] Absolute paramagnetic shift, see text. [b] See text. [c] Calculated from ref 18 with eq 7.

Table III. Kondo–Yamashita Analysis of the Chemical Shift Data for the Alkaline Earth Sulfides and PbS

compd	$-\sigma_p$,[a] ppm	E_r,[b] eV	Δ'', eV	$10^2 E_r^{-1}\Delta''^{-1}$, eV^{-2}
MgS	312	114	6.6[c]	3.07
CaS	457	107	5.4	4.02
SrS	528	106	4.8	4.51
BaS	777	89	3.9	6.60
PbS	189	132	*d*	*d*

[a] Absolute paramagnetic shift, see text. [b] From ref 71. [c] Estimated from systematic trends in the II–VI series. [d] Energy value Δ'' not relevant for present calculations.

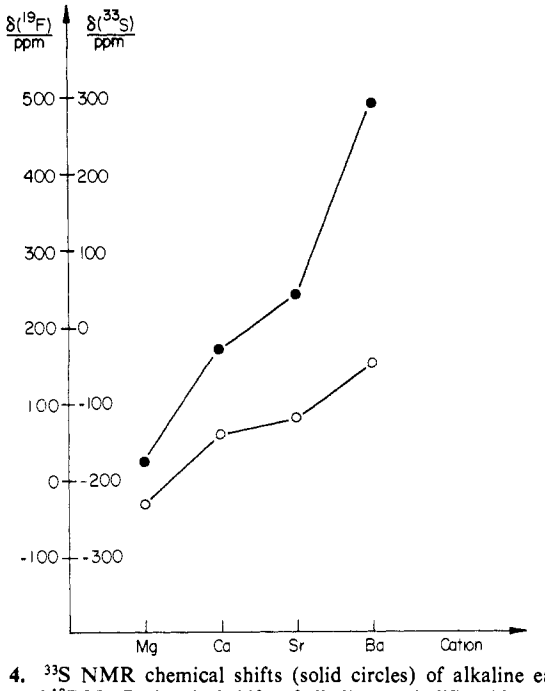

Figure 4. ^{33}S NMR chemical shifts (solid circles) of alkaline earth sulfides and ^{19}F NMR chemical shifts of alkaline earth difluorides (open circles, ref 26) vs. cation. Shift references are CS_2 and C_6F_6, respectively.

(50) Bredig, M. A. *J. Phys. Chem.* **1942**, *46*, 747.
(51) Lipson, H.; Beevers, C. A. *Proc. R. Soc. London Ser. A* **1935**, *148*, 664.
(52) Sahl, K. *Beitr. Mineral. Petrog.* **1963**, *9*, 111.

to obtain a value for the paramagnetic contribution σ_{para}. The absolute paramagnetic shieldings thus calculated for the post-transition-metal sulfides are listed in Table II. The calculated σ_{para} for Li_2S (−138.7 ppm) is the smallest such value in any sulfur compound yet observed.

Large chemical shift differences are found for the rocksalt type sulfides. As shown in Figure 4 the alkaline earth sulfide shifts become increasingly paramagnetic as the cation size is increased. This trend compares very well with the large anion shift differences noted for other highly ionic lattices, such as the rocksalt type IIa oxides[22] and Ia halides,[23-25] as well as the fluorite type IIa difluorides[26] which are included in Figure 4. Also, the relative order of the chemical shifts in ZnS, CdS, and PbS correlates well with the ^{77}Se and ^{125}Te results obtained by other authors.[21,27-29] However, the relative variation of the alkaline earth sulfide shifts with respect to those of the post-transition-element sulfides requires further consideration. As will be outlined in the following, the observed chemical shifts reflect the combined effect of two separate phenomena, anion–cation overlap and covalency.

Model calculations reveal that in eq 2 only shielding effects arising from electrons centered on the atom in question need to be considered[55] and that for all nuclei except hydrogen the second term generally dominates the chemical shift trends. The discussion which follows will therefore neglect changes in the σ_{dia} term, which are expected to be small within the series of sulfides. The σ_{para} term describes the paramagnetic shift arising from the angular momentum of excited atomic states which are mixed into the ground state and can be expressed in terms of a LCAO–MO framework as arising from valence electron imbalances P_u and D_u in the p and d orbitals, respectively, of the atom under consideration:[55]

$$\sigma_{para} = \frac{-\mu_0 e^2 \hbar^2}{6\pi m^2} \Delta^{-1} [\langle r^{-3} \rangle_p P_u + \langle r^{-3} \rangle_d D_u] \quad (3)$$

In this equation, m and e denote the electron mass and charge, μ_0 is the magnetic permeability of the vacuum, and Δ is an average excitation energy involving summation over all excited states, which is frequently approximated by the excitation energy of the lowest transition. The expectation value of the inverse cube of the electron–nucleus distance, $\langle r^{-3} \rangle_p$, can be taken from atomic data[56] and amounts to 3.37×10^{31} m^{-3} for the ^3P atomic state of sulfur. Since the 3d orbitals of sulfur are unoccupied and, in the bonding description of the compounds under study, s–p–d hybridization is generally not invoked, the participation of d states will be neglected here. Furthermore, we assume that within this series of chemically closely related compounds the variations in $\langle r^{-3} \rangle_p$ are small compared to changes in the P_u term. We will thus restrict the following discussion to the electron imbalance of the 3p orbitals (which would be zero for an isolated S^{2-} ion) and the Δ^{-1} term.

Chemical Shifts of ZnS, CdS, and PbS. The discussion of the tetrahedral solids ZnS and CdS follows the bond orbital model developed by Harrison and co-workers.[19,20] Four sp^3 wave functions of the anions and cations, $|h^a\rangle$ and $|h^c\rangle$, respectively, are combined to form four bonding orbitals, b:

$$b = u_a|h^a\rangle + u_c|h^c\rangle$$

Minimization of the bond energy

$$E_b = \frac{\langle b|H|b\rangle}{\langle b|b\rangle}$$

by variation of the coefficients u_a and u_c yields the result

$$u_i^2 = \frac{1}{2}\left(\frac{1 - S(1-\alpha_p^2)^{1/2}}{1 - S^2} \pm \frac{\alpha_p}{(1-S^2)^{1/2}} \right) \quad (4)$$

where the plus and the minus signs refer to the anion and the cation, respectively. In eq 4, α_p represents the polarity of the bond, which is defined according to

$$\alpha_p = \frac{V_3}{(V_2^2 + V_3^2)^{1/2}}$$

where V_3 and V_2 are the heteropolar and the homopolar contributions to the total bonding energy, respectively. The overlap S between the anion and cation wave functions is given by

$$S = \langle h^a|h^c\rangle$$

In the LCAO–MO framework, eq 3 can be written as

$$\sigma_p = \frac{-\mu_0 e^2 \hbar^2}{\pi m^2} \Delta^{-1} \langle r^{-3} \rangle_p [u_i^2(1 - u_i^2)] \quad (5)$$

where the u_i represent coefficients for both anions and cations.[58] Equations 4 and 5 imply that σ_p may change as a result of variations in both α_p and S. Neglecting S as a first approximation would lead for both anion and cation to

$$\sigma_p = \frac{-\mu_0 e^2 \hbar^2}{4\pi m^2} \Delta^{-1} \langle r^{-3} \rangle_p (1 - \alpha_p^2) \quad (6)$$

which predicts an increase in σ_p with decreasing bond polarity.

It is shown in ref 27 that the tight binding approach used for tetrahedrally coordinated solids can be extended to include IV–VI compounds as well. Thus we will include PbS, which crystallizes in the rocksalt structure, in the following discussion of the chemical shift trends. In order to test the validity of the approximate eq 6, data for the ionicities are needed. Attempts to correlate the observed ^{33}S chemical shift data solely with Pauling,[13] Mulliken,[14] or Gordy[15] electronegativities were not successful. However, the Phillips–Van Vechten definition of a crystal ionicity f_i on the basis of experimentally observed dielectric constants[16-18] is expected to be more appropriate for predicting NMR chemical shifts in the solid state. It is shown in ref 19 that a direct relationship of f_i with Harrison's bond polarity parameter α_p exists:

$$f_i = 1 - (1 - \alpha_p^2)^{3/2} \quad (7)$$

The data in Table II reveal that the absolute paramagnetic shifts deduced from the experimental data are indeed proportional to $(1 - \alpha_p^2)$, hence suggesting that the variations in S and Δ are either small for the compounds under consideration or result in a fortuitous mutual cancellation effect. While for IV–IV and III–V compounds theoretical values for S, obtained within the framework of an extension of the bond orbital model, have been tabulated,[57] no such values are available for the compounds under discussion. In principle, the numerical value of the overlap could be determined by applying eq 4 to our data, provided an exact value of Δ were known. However, large uncertainties are usually associated with this energy parameter, hence rendering absolute predictions of paramagnetic shifts ambiguous in general. Thus it seems more appropriate to estimate Δ from our measurements, utilizing Harrison's values for α_p and reasonable boundary conditions for S. The latter can be obtained from the considerations which follow.

The variation of the function $u^2(1 - u^2)$ with α_p and S is shown in Figure 5. In general, one procedure to estimate differences in overlap is to measure the temperature dependence of σ_p. As pointed out by Becker,[58] S is expected to increase with temperature, reflecting the increase of the vibrational amplitudes. Consequently, the sign of the temperature coefficient can give an upper and a lower limit for the overlap. For the present compounds, this parameter is positive, thus restricting S to values between zero and 0.26, 0.25, and 0.23 for ZnS, CdS, and PbS, respectively. The upper and lower limits of Δ calculated from this procedure are listed in Table II, along with all parameters used. The values are in a reasonable range, being intermediate

(53) Gierke, T. D.; Flygare, W. H. *J. Am. Chem. Soc.* **1972**, *94*, 7277.
(54) Ramsey, N. F. *Phys. Rev.* **1950**, *78*, 669.
(55) Jameson, C. J.; Gutowsky, H. S. *J. Chem. Phys.* **1964**, *40*, 1714.
(56) Barnes, R. G.; Smith, W. V. *Phys. Rev.* **1954**, *93*, 95.
(57) Huang, C.; Moriarty, J. A.; Sher, A. *Phys. Rev.* **1976**, *14*, 2539.
(58) Becker, K. D. *J. Chem. Phys.* **1978**, *68*, 3785.

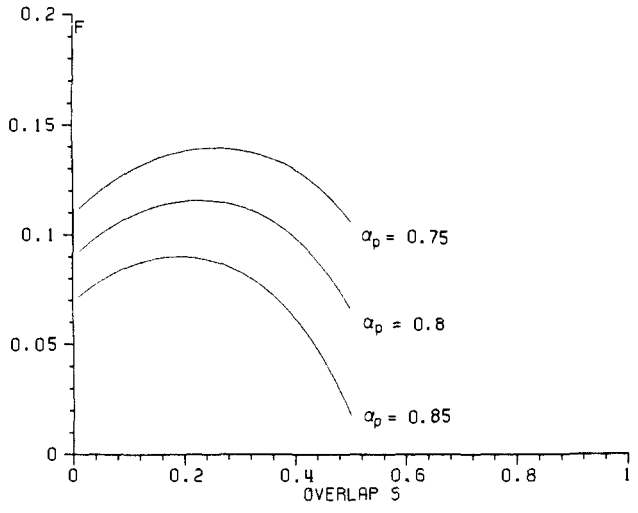

Figure 5. Plot of $F = u^2(1 - u^2)$ vs. overlap S for three different values of α_p. After ref 58.

between the respective optical band gaps[59] and Harrison's bonding energies[19] $2(V_2^2 + V_3^2)^{1/2}$ (which coincide with the energy E_2 in the optical spectrum). Thus the calculations performed above lend credence to the absolute chemical shift scale proposed by Wasylishen and co-workers.[36]

Chemical Shifts of MgS, CaS, SrS, and BaS. While the crystalline ionicities f_i reflect the chemical shift trends for the covalently bonded post-transition-metal sulfides correctly, they predict the opposite of what is found experimentally within the highly ionic alkaline earth sulfide series (f_i = 0.79, 0.90, and 0.91 for MgS, CaS, and SrS, respectively;[17] no value is given for BaS). Similarly, the above concept is unsuccessful in accounting for chemical shift trends in alkali, copper, and alkaline earth halides[23-26,30,31] as well as in a variety of III–V compounds.[32-35] Since the alkaline earth sulfides represent ionic, octahedrally coordinated solids, application of the bond orbital model is not appropriate. Unfortunately, for compounds crystallizing in the rocksalt structure, the influence of partial covalency and anion–cation overlap have been treated only separately,[24,25] and no comprehensive theory exists. However, it was found that for the alkali halides both the quadrupolar spin–lattice relaxation times as well as the pressure and temperature dependencies of the chemical shifts are in better agreement with the overlap model[60-62] than the covalency model. Also, theoretical calculations for the alkali halide series reveal that with increasing size of the ions the anion–cation overlap increases,[63,64] while the anion–anion overlap decreases, their combined effect accounting for the observed chemical shift trends in these compounds.[60,62,65] We will therefore restrict our discussion to differences in anion–cation and anion–anion overlap and neglect the influence of covalency. The paramagnetic shift is given by the expression of Kondo–Yamashita[24]

$$\sigma_p = -\frac{16}{3}\frac{\mu_0}{\pi}\frac{e^2\hbar^2}{m^2}Z\langle r^{-3}\rangle_p\frac{\Lambda}{\Delta'} \qquad (8)$$

where Z is the number of nearest neighbors, Δ' is an average excitation energy of the ionic state (somewhat differently defined as compared to eq 3), and Λ denotes the sum of squares of overlap integrals between an outermost p orbital of the sulfur atom and the orbitals of the nearest and next-nearest neighbor ions. The other symbols have their previously defined meanings. Since for the compounds under discussion these overlap integrals have not yet been evaluated, we will not attempt an absolute calculation of the chemical shift but will instead limit our discussion to the ability of the ionic Kondo–Yamashita approach to predict the chemical shift trend observed within this group of compounds. As mentioned above, Λ generally increases with the ionic size, and previous empirical correlations of chemical shifts with interatomic distances have dwelled on this relationship.[22,66-68] A more direct measure of Λ has been pointed out by Baron,[61] who suggests that the overlap should be proportional to the sum E_r of the repulsive anion–cation and anion–anion overlap energies, values which are calculable within the framework of the Born–Mayer theory.[69] While this is true when changes in the overlap for a given compound are considered as a function of temperature or pressure, the inverse dependence is expected if overlap variations within a series of compounds at their equilibrium interatomic distances are under discussion. In this case, one would expect the extent of the overlap to *increase* as the overlap repulsive energy between the constituent ions *decreases*. This view is supported by a comparison of E_r values calculated by Cubicciotti[70] with the overlap integrals evaluated quantum-mechanically by Löwdin[63] and Hafemeister and Flygare,[64] which shows that the proportionality is actually inverse. A similar reversal has been noted by Sears[23] in a study of the ^{19}F NMR chemical shifts of alkali fluorides. Likewise, Figure 6, which shows a plot of σ_p vs. E_r data for the present compounds,[71] suggests an inverse correlation, which was found to include even the chemically very different lead sulfide. Following the argumentation outlined above, this result indicates that overlap effects, especially between anion and cation, play an important role in determining the chemical shift trend.

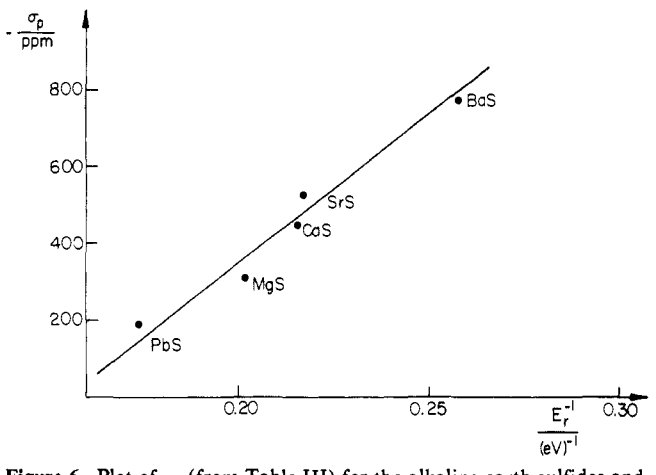

Figure 6. Plot of σ_p (from Table III) for the alkaline earth sulfides and PbS vs. the inverse overlap repulsion energy E_r calculated from the Born–Mayer theory.

Independent qualitative confirmation of the role of overlap comes from the sign of the chemical shift temperature coefficients (see Table I). In alkali halides, this parameter is positive, hence indicating that the increase in the variational amplitudes overrides the effect of thermal dilation, resulting in a net increase of the overlap.[62] The same behavior is found for the present compounds. Although it is not possible to obtain values of Λ from these coefficients, it is worth noting that a distinct correlation exists: large paramagnetic shifts are associated with small temperature coefficients and vice versa.

Finally it should be pointed out that the correlation suggested by Figure 6 should be improved if the trend of the average excitation energy parameter Δ' within this group of compounds is taken into account. Unfortunately, this parameter is a complicated

(59) Landolt-Börnstein, "Numerical Data and Functional Relationships", In "Science and Technology, New Series"; Madelung, O., Ed.; Springer-Verlag: Berlin, Heidelberg, New York, 1982; Vol. 17b.
(60) Yamagata, Y. *J. Phys. Soc. Jpn.* **1964**, *19*, 10.
(61) Baron, R. *J. Chem. Phys.* **1973**, *38*, 173.
(62) Ngai, L. H. *J. Phys. Chem. Solids* **1969**, *30*, 571.
(63) Löwdin, P. O. *Adv. Phys.* **1956**, *5*, 1.
(64) Hafemeister, D. W.; Flygare, W. H. *J. Chem. Phys.* **1965**, *43*, 795.
(65) Hafemeister, D. W.; Flygare, W. H. *J. Chem. Phys.* **1966**, *44*, 3584.
(66) Sears, R. E. J. *J. Chem. Phys.* **1973**, *59*, 973.
(67) Sears, R. E. J. *J. Chem. Phys.* **1978**, *69*, 4321.
(68) Boden, N.; Kahol, P. K.; Mee, A.; Mortimer, M.; Peterson, G. N. *J. Magn. Reson.* **1983**, *54*, 419.
(69) Born, M.; Mayer, J. E. *Z. Phys.* **1932**, *75*, 1.
(70) Cubicciotti, D. *J. Chem. Phys.* **1959**, *31*, 1646.
(71) Bakhshi, P. S.; Jain, V. K.; Shanker, J. *J. Inorg. Nucl. Chem.* **1981**, *43*, 901.

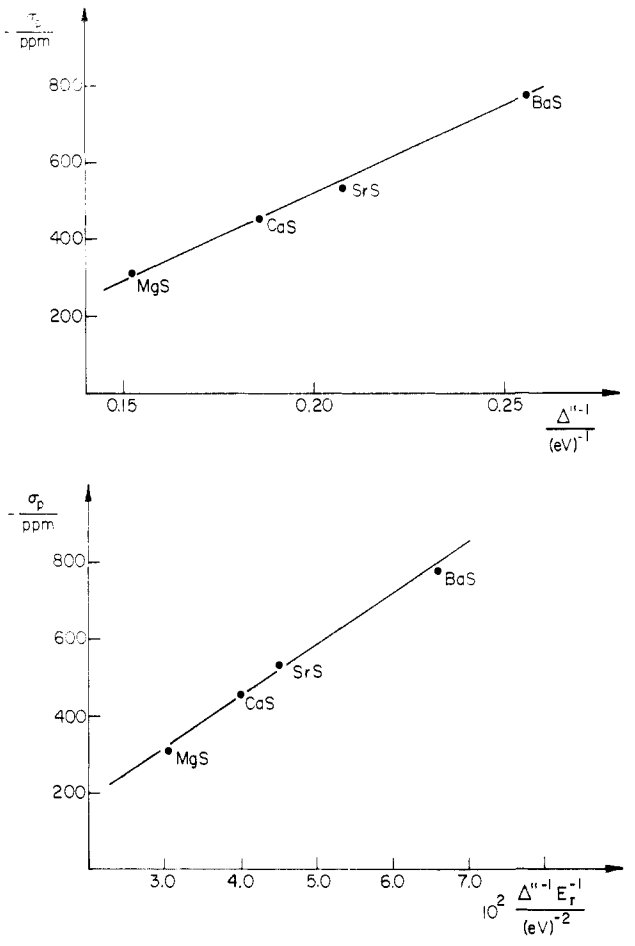

Figure 7. (a) Plot of σ_p (from Table III) vs. the inverse of Δ'', the energy of the first optical absorption maximum for the alkaline earth sulfides. (b) Plot of σ_p (from Table III) vs. $1/\Delta''E_r$ for the alkaline earth sulfides.

average and does not relate directly to experimental observables. Studies of group IIa chalcogenides, however, have shown a regular red shift of the overall optical and UV absorption pattern as the cation size is increased.[72-74] In the absence of quantative knowledge of Δ', we take the variations in the first absorption maxima Δ'' in the present compounds as a measure of the variations in Δ'. Figure 7 demonstrates that both $1/\Delta''$ as well as $1/\Delta''E_r$ are approximately linearly correlated with σ_{para}. Although these correlations are noteworthy, their exact theoretical functional form may be more involved. (Indeed, the three plots of Figures 6 and 7 *cannot* be simultaneously linear, although over a limited range they do appear so.) Also, it should be mentioned that parts a and b of Figure 7 exclude PbS, since the electronic structure of this compound is fundamentally different from that of the IIa sulfides, and thus the first electronic absorption maximum relates to Δ' in a different manner.

Although dependencies analogous to those described above also have been noted experimentally for the alkali fluoride series,[23] the relative success of the extended Kondo–Yamashita approach outlined here is certainly noteworthy for the present sulfides, since considerable covalency effects are expected for these compounds. Despite this qualitative agreement, it would be worthwhile to formulate a theory which includes the influence of both overlap and covalency effects on the paramagnetic shift, e.g., within the framework of a tight binding approach analogous to the bond orbital model. Such a theory should be capable of explaining the variations of the chemical shifts *among the different structural types* of metal sulfides, which have primarily been discussed separately in this paper.

Conclusions and Future Prospects

We have shown that solid-state NMR of ^{33}S in sufficiently symmetric environments is feasible provided that (a) a very high magnetic field is used to minimize second-order quadrupole broadening and (b) artifacts in the free induction decay resulting in a "rolling base line" are suppressed by use of a RIDE pulse sequence. The performance of the original sequence can be significantly improved by incorporating composite 180° pulses.

The small chemical shift range in the solid sulfates limits the application of ^{33}S NMR in this class of compounds to the observation of differences in quadrupole coupling constants. On the other hand, the large chemical shift range observed for the metal sulfides suggests that the method has great potential for applications in the study of systems containing mixtures or solid solutions of inorganic sulfides. Such systems are important from both materials science and geochemical standpoints. Furthermore, the availability of isotopically enriched ^{33}S might enable studies of metal sulfides on the surfaces of technologically important catalysts to be carried out. Although the relatively low sensitivity of detection and relatively broad line widths may limit some applications, the use of larger sample volumes, higher pulse power, and magic- and variable-angle sample spinning can be expected to yield significant improvements and to extend the range of compounds which can be investigated.

The chemical shift trends observed for ^{33}S in solids can be rationalized in terms of the existing calculational approaches. While for the more covalently bonded post-transition-metal sulfides the bond orbital model can be applied and changes in bond ionicity seem to dominate the observed trend, the alkaline earth sulfide shifts are best described by an extended Kondo–Yamashita approach including next-nearest neighbor interactions. In order to obtain a more quantitative description for the latter, pressure-dependent chemical shift data are needed. Nevertheless, the present study should serve to disperse the aura of pessimism which in the past has surrounded the possibility of studying ^{33}S NMR in solids.

Acknowledgment. This research was carried out at the Southern California Regional NMR Facility, funded by NSF Grant CHE 84-40137. We thank Prof. George Rossman for providing a variety of mineral samples and gratefully acknowledge valuable discussions with Prof. Sunney I. Chan.

Registry No. Li_2S, 12136-58-2; Na_2S, 1313-82-2; MgS, 12032-36-9; CaS, 20548-54-3; SrS, 1314-96-1; BaS, 21109-95-5; PbS, 1314-87-0; ZnS, 1314-98-3; CdS, 1306-23-6; K_2SO_4, 7778-80-5; Rb_2SO_4, 7488-54-2; Cs_2SO_4, 10294-54-9; Tl_2SO_4, 7446-18-6; $(NH_4)_2SO_4$, 7783-20-2; $KAl(SO_4)_2 \cdot 12H_2O$, 7784-24-9; $RbAl(SO_4)_2 \cdot 12H_2O$, 7784-29-4; $CsAl(SO_4)_2 \cdot 12H_2O$, 7784-17-0; $NH_4Al(SO_4)_2 \cdot 12H_2O$, 7784-26-1; $TlAl(SO_4)_2 \cdot 12H_2O$, 13477-85-5; thenardite, 13759-07-4; glauberite, 13767-89-0; bloedite, 15083-77-9; anhydrite, 14798-04-0; gypsum, 13397-24-5; baryte, 13462-86-7; sulfur-33, 14257-58-0.

(72) Zollweg, R. J. *Phys. Rev.* **1958**, *111*, 113.
(73) Saum, G. A.; Hensley, E. B. *Phys. Rev.* **1959**, *113*, 1019.
(74) No reliable experimental data are available for MgS. The value given in Table III was estimated by extrapolating the trends observed in ref 72 and 73.